J Mater Sci (2010) 45:3707–3713
DOI 10.1007/s10853-010-4383-x

Synthesis, characterisation and thermal behaviour of lithium aluminosilicate inorganic polymers

Sean J. O'Connor · Kenneth J. D. MacKenzie

Received: 20 November 2009 / Accepted: 3 March 2010 / Published online: 14 May 2010

Abstract Lithium aluminosilicate inorganic polymers were synthesised from dehydroxylated kaolin-type clay (halloysite) by the conventional method under highly alkaline conditions with lithium hydroxide or lithium silicate solutions of two different Li_2O/SiO_2 molar ratios. Variants were also developed of a solid-state synthesis method involving the thermal reaction of dehydroxylated halloysite with LiOH followed by hydration of the product. The molar compositions of the materials prepared by all three methods ($SiO_2/Al_2O_3 = 2.41$–3.27, $Li_2O/SiO_2 = 0.30$–0.61, and $H_2O/Li_2O = 9.33$–10.40) fall within the range of compositions previously reported to produce viable geopolymers. Curing at 40 °C produces solid samples of varying viability depending on the amount of synthesis water. The cured materials are not characteristically X-ray amorphous, but contain the lithium zeolites Li-ABW and fibrous Li-EDI, the latter in the materials synthesised by solid-state reaction. The ^{27}Al and ^{29}Si MAS NMR spectra of the cured materials contain narrow resonances more characteristic of zeolites than of inorganic polymers. Heating the synthesised products at <800 °C produces β-eucryptite, $LiAlSiO_4$. In a further series of thermal reactions, β-spodumene, $LiAlSi_2O_6$ is formed at 900 °C, decomposing at 1100 °C to form additional β-eucryptite. At 1275 °C, β-spodumene reappears in the samples of higher silica content. Judicious manipulation of the composition and thermal treatment of the Li-zeolites formed in these lithium aluminosilicate syntheses could make them useful precursors to β-eucryptite and β-spodumene ceramics.

Introduction

Inorganic polymers (otherwise known as geopolymers) are typically X-ray amorphous aluminosilicate materials formed by reacting a solid aluminosilicate source such as dehydroxylated kaolinitic clay (metakaolin) with an alkali silicate solution under highly alkaline conditions [1]. These materials cure and harden at ambient temperatures to form a tetrahedral network in which charge balance is achieved by the presence of the alkali metal cations, most commonly Na^+ or K^+ [2]. The formation of viable Li^+ geopolymers by this method is difficult, probably because of the lower reactivity of lithium silicate solutions, resulting in the much slower dissolution of solid silica by lithium silicate or LiOH than is the case with Na or K [3, 4]. Furthermore, lithium silicate solutions display higher degrees of silicate polymerisation and are slower than the other alkali silicates to re-equilibrate in response to changes in the concentration of silica, lithium or water [3, 5].

Dissolution of metakaolin in alkaline solutions of alkali metal silicates results in the formation of either geopolymers or zeolites, depending on the reaction conditions [1, 6]. The reaction products are determined by the concentrations of dissolved silica and alumina, the reaction temperature and the identity of the alkali ion [7]. In general, where silica and alumina are present in very high concentrations and the concentration of dissolved silica is in excess of alumina (i.e. $[SiO_2]/[Al_2O_3] > 2.5$), X-ray amorphous geopolymers are formed [1, 2, 6, 8], whereas under other conditions, crystalline zeolites are reported to form [7, 9].

S. J. O'Connor · K. J. D. MacKenzie (✉)
MacDiarmid Institute for Advanced Materials
and Nanotechnology, School of Chemical and Physical
Sciences, Victoria University of Wellington, P.O. Box 600,
Wellington, New Zealand
e-mail: kenneth.mackenzie@vuw.ac.nz

Because of these differences between the chemistry of the silicates of Li and the other alkali metals, successful synthesis of Li^+ aluminosilicates with the characteristics of conventional geopolymers by the usual synthesis reaction of dehydroxylated kaolinite with lithium silicate solutions has not been reported. However, Kolusek et al. [10] have suggested an alternative to the conventional geopolymer synthesis route involving solid-state reaction between an undehydroxylated clay mineral and the alkali hydroxide to give a hydraulically active product that sets upon the addition of a small amount of water. This solid-state method has successfully been adapted to synthesise gallioogermanate inorganic polymers [11], and was applied to the lithium aluminosilicate system described here.

The successful development of a convenient synthesis route for such lithium compounds could have potential applications in the preparation of precursors for important crystalline ceramic phases such as β-spodumene ($LiAlSi_2O_6$) and β-eucryptite ($LiAlSiO_4$). β-eucryptite and β-spodumene ceramics have excellent resistance to thermal shock as a result of the near zero or negative thermal expansion coefficients of the two component phases [12, 13]. Lithium zeolites have occasionally been considered as precursors for these phases [14, 15].

The aim of this study is to prepare compounds in the lithium aluminosilicate system from dehydroxylated clay by three methods, the conventional geopolymer synthesis, the solid-state synthesis method and a modification of the solid-state method. The resulting monolithic products were identified and structurally characterised by XRD, SEM and solid-state MAS NMR, and their thermal behaviour determined to assess their potential as precursors for lithium aluminosilicate ceramics.

Experimental

The starting material was halloysite, a New Zealand kaolin-type clay (Imerys Premium Grade) which was dehydroxylated at 570 °C overnight. This clay contains quartz and cristobalite as impurities, giving it the molar composition $SiO_2/Al_2O_3 = 2.41$, based on the supplier's analytical data. Two lithium silicate solutions used in the conventional synthesis method were produced by reacting lithium hydroxide with silicic acid (J.T. Baker Reagent Grade) in water for 6 days. Shortly before use, sufficient additional lithium hydroxide was added to the solutions to produce two solutions of Li_2O/SiO_2 molar composition 4.55 and 2.15. These solutions were used in the conventional synthesis to prepare samples C2 and C3, respectively. For comparison, another sample, C1, was prepared by the conventional method using a solution of LiOH only.

Lithium silicate powders of four different Li_2O/SiO_2 molar ratios for use in a modification of the solid-state synthesis method were prepared by heating silica fume (Elkem 971-U) with lithium hydroxide (BDH reagent Grade) at 600 °C overnight, followed by several cycles of regrinding and re-heating to ensure complete solid-state reaction and homogeneity of the product. The Li_2O/SiO_2 molar ratios of these solid silicates, used to prepare samples M1, M2, M3 and M4 were 1.98, 1.63, 1.36 and 1.16, respectively. XRD showed these lithium silicate powders to contain two polymorphs of Li_4SiO_4 (PDF no. 37-1472 and PDF no. 74-3473) and Li_2SiO_3 (PDF no. 29-0828), the relative XRD peak heights of Li_4SiO_4 decreasing with increasing silica content.

Sample synthesis by the conventional geopolymer method

In this synthesis, dehydroxylated halloysite was thoroughly mixed with the LiOH or lithium silicate solution prepared as above, in proportions corresponding to the three compositions C1, C2 and C3 (Table 1). Table 1 shows that the molar compositions of all the samples, including those prepared by the solid state methods, are close to those reported to be optimal for the formation of sodium geopolymers ($SiO_2/Al_2O_3 = 3.3$–3.8, $Na_2O/SiO_2 = 0.25$–0.45, $H_2O/Na_2O = 10$–17.5) [2]. The mixtures were placed into polyethylene moulds, sealed with plastic film and cured at 40 °C for 3 days to form hard, durable monolithic samples.

Table 1 Molar compositions of the samples

Synthesis method	Sample	Li_2O/Al_2O_3	SiO_2/Al_2O_3	Li_2O/SiO_2	H_2O/Li_2O
Conventional	C1	1.48	2.41	0.61	9.65
Conventional	C2	1.47	2.73	0.54	9.70
Conventional	C3	1.48	3.09	0.48	9.62
Solid state	S	1.03	2.41	0.43	10.40
Modified solid state	M1	1.03	2.93	0.35	9.33
Modified solid state	M2	1.02	3.04	0.34	9.64
Modified solid state	M3	1.00	3.15	0.32	9.76
Modified solid state	M4	1.00	3.27	0.30	9.97

Sample preparation by solid state synthesis

Sample S (Table 1) was synthesised by the solid-state method [10] in which a mixture of dehydroxylated halloysite and lithium hydroxide in the appropriate proportions was reacted at 550 °C for 4 h. The SiO_2/Al_2O_3 molar ratio of this sample (2.41) is determined solely by the composition of the clay, since the method provides no additional Al source. The resulting powder was then hydrated by the addition of water to form a paste of the composition shown in Table 1 which was placed in moulds, sealed and cured as above.

In a modification of the solid-state synthesis method, the solid lithium silicate powders prepared as above were dry-mixed with dehydroxylated halloysite and hydrated by the addition of sufficient water to give the sample compositions M1–M4 (Table 1).

Thermal treatment of cured samples

Pieces of the cured and hardened samples were heated in air in an electric furnace at 10 °C min^{-1} to 800, 900, 1100 and 1275 °C and held at these temperatures for 8 h.

Characterization of the products

The heated and unheated samples were powdered and examined by XRD (Philips PW1700 with computer-controlled goniometer and graphite monochromator using Co Kα radiation) and ^{27}Al and ^{29}Si MAS NMR spectroscopy at 11.7T (Bruker Avance 500 spectrometer) under the following conditions:

^{27}Al: 1s (π/10 pulse for solution) with a 1s delay, using a 4-mm Doty MAS probe spun at 10–12 kHz, the spectra referenced to $Al(H_2O)_6^{3+}$.

^{29}Si: 6 µs (π/10) pulse with a 30s delay, using a 5-mm Doty MAS probe spun at 5–6 kHz, the spectra referenced to TMS. The fractured surfaces of selected samples were coated with platinum and examined using a JEOL6500 FEG-SEM.

Results and discussion

All the present samples set satisfactorily, but their cured strength depended on the water content; only those samples with H_2O/Li_2O molar ratios lying within the range ~9.0–10.0 formed strong monoliths. Samples with water contents outside this range were more fragile and crumbly.

The X-ray diffractograms of selected cured samples are shown in Fig. 1. None of the synthesised compounds show significant intensity in the region characteristic of the X-ray amorphous diffraction pattern of an inorganic polymer (d = 3.05–3.3 Å, [1]. However, all contain crystalline features corresponding to lithium zeolites, in addition to small amounts of quartz and cristobalite impurities from the clay starting material. The principal zeolite phase present in all the three compounds prepared by the conventional synthesis is Li-ABW (PDF no. 027-1211), with a small amount of Li_2CO_3 (PDF no. 01-72-1216) also present in sample C1 and a small amount of zeolite Li-EDI (PDF no. 01-79-1893) present in sample C3. By contrast, zeolite Li-EDI (PDF no. 01-79-1893) was the principal phase present in the samples synthesised by the solid-state methods. Li-EDI is a fibrous zeolite with the edingtonite (EDI) framework structure [16] and its content in the samples, reflected by the relative XRD peak heights, decreased from sample S through samples M1–M3. Sample M4 contained only traces of zeolite Li-EDI but its XRD diffractogram showed the presence of small amounts of

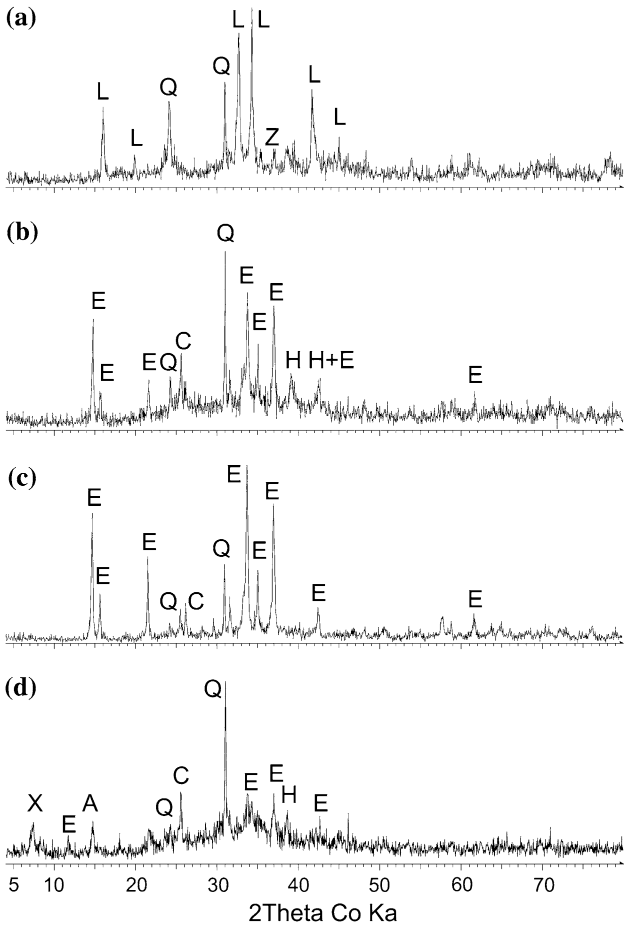

Fig. 1 Typical XRD diffractograms of as-synthesised cured lithium inorganic polymers. **a** Sample C1, **b** sample S, **c** sample M1, **d** sample M4. *Q* quartz (PDF no. 33-1161), *C* cristobalite (PDF no. 39-1425), *L* Li-zeolite ABW (PDF no. 27-1211), *E* Li zeolite EDI (PDF no. 01-79-1893), *H* $LiOH{\cdot}H_2O$ (PDF no. 25-486), *X* Li zeolite X (PDF no. 38-236), *A* Li zeolite A (PDF no. 38-241), *Z* zabuyelite, Li_2CO_3 (PDF no. 01-72-1216)

Li-zeolite A (PDF no. 38-0241) and Li-zeolite X (PDF no. 38-0236). A small amount of residual $LiOH{\cdot}H_2O$ (PDF no. 25-486) is also present in sample S. Thus, although all the three synthetic methods produce zeolitic phases, only those synthesised by the conventional method in which the Li_2O/Al_2O_3 molar ratio is relatively high (1.48) form Li-ABW. The solid-state syntheses, in which the Li_2O/Al_2O_3 molar ratios are 1.0–1.03, form the fibrous Li-EDI, reflecting the lower alkalinity imposed on these systems by the synthesis method.

The formation of Li-EDI in many of the hardened samples was unexpected since the product of reaction between LiOH and metakaolin has previously been reported to be Li-ABW [7]; although, mixed Na,Li and K,Li-zeolites with the edingtonite structure (designated Na,Li-F and K,Li-F) have been reported [7]. The only previous reported formation of pure Li-EDI has been by hydrothermal synthesis of an aluminosilicate sol [17] and by microwave treatment of the amine precursors silatrane with alumatrane [18]. The preferential formation of Li-EDI may be favoured by the low pH of the present synthesis conditions, as previous reports of Li-ABW formation have usually involved Li_2O/Al_2O_3 ratios greater than 1.5 [7, 19]. However, the present results are in good agreement with one previous patent [20]. Sample C3 contains both Li-EDI and Li-ABW zeolites, whereas the less silicaceous (more alkaline) samples C1 and C2 form only Li-ABW.

The behaviour of the present Li-aluminosilicate geopolymer system differs from that of the Na-aluminosilicate system, which does not normally form zeolites with the fibrous edingtonite-type structure, for example by reaction of metakaolinite with NaOH [7]. However, edingtonite-type zeolite Na–F has been reported to form in a flyash-derived sodium aluminosilicate geopolymer gel seeded with nanoparticles of Al_2O_3 [21]; this is suggested to be due to the catalytic effect of the seed particles on gel formation and phase separation. By contrast, with the Na aluminosilicate system, edtingtonite-type K–F zeolite forms readily by hydrothermal synthesis from aluminosilicate gels, kaolinite or metakaolinite [7].

The growth and interlocking of these zeolite crystals is probably responsible for the strength development in the present materials. The water content of the original mixture appears also to be crucial for this strength development, since this can be poor even in samples that contained sufficient water to promote zeolite formation. Little or no volume change was observed in the samples as they set, probably because the volume of the interlocking zeolite crystals is similar to that of the dehydroxylated halloysite and water reactants.

An increase in the silica content significantly decreases the size of the zeolite crystallites formed and the amount of crystalline content in the samples as observed by SEM and XRD. This is probably due to the fact that for a given alkali content, an increase in the amount of dissolved silica results in a higher SiO_2/Li_2O ratio and thus a lower pH of the reaction mixture, hindering dehydroxylated halloysite dissolution. At the highest silica contents, the pH is relatively low and the correspondingly large amount of dissolved silica results in the formation of zeolites A and X. This is supported by other experiments (not shown here) in which the lithium content was decreased to a molar ratio of $Li_2O/Al_2O_3 = 0.4–1.0$ without increasing the amount of silica, resulting in the formation of less Li-EDI and no zeolites A or X.

A selection of typical SEM micrographs of the cured samples is shown in Fig. 2 which indicates that the decrease in amount of the zeolitic phase is accompanied by an increasingly irregular microstructure. The microstructure of the conventionally synthesised samples (Fig. 2a) consists largely of crystalline particles of irregular shape and size. Samples S (Fig. 2b) and M1 (Fig. 2c) consist of quite regular spherical structures approximately 10 μm in size which are seen at higher magnification (Fig. 2e, f) to be prismatic plates (in sample M1) or rods (in sample M3). Samples M2–M5 contain increasing amounts of apparently amorphous agglomerates, with decreasing amounts of rods dispersed throughout.

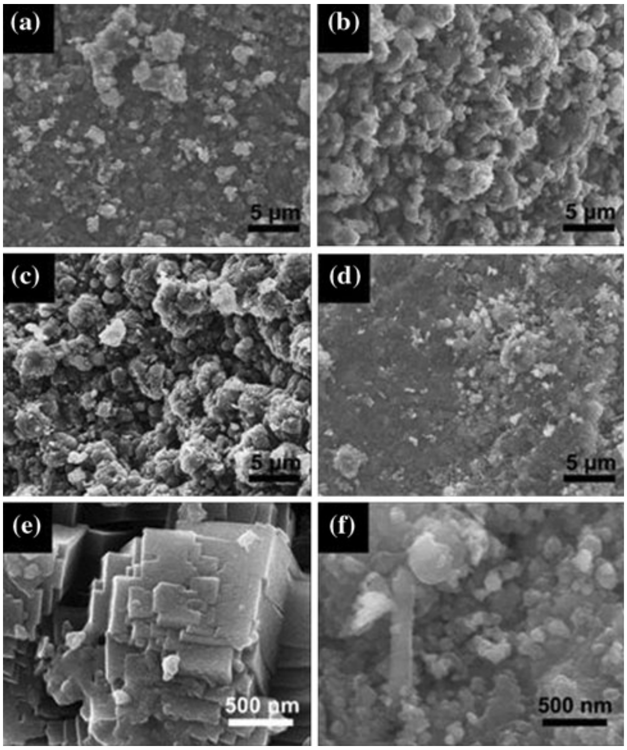

Fig. 2 SEM images of as-synthesised cured lithium inorganic polymers. **a** Sample C1, **b** sample S, **c** sample M1, **d** sample M4, **e** sample M1, **f** sample M3

NMR spectroscopy

Representative ^{27}Al and ^{29}Si MAS NMR spectra of the cured products of the three synthesis methods are shown in Fig. 3. The ^{27}Al MAS NMR spectra of the products synthesised by all the three methods contain a principal resonance at about 60 ppm corresponding to Al in tetrahedral coordination (Fig. 3a–d). Since this is the coordination state of Al in both X-ray amorphous geopolymers [2] and zeolites, this result does not distinguish between these products, but taken in conjunction with the XRD results for these samples, these spectra are consistent with the formation of zeolites.

The characteristic broad ^{29}Si MAS NMR geopolymer resonance centred at about −90 ppm [2] does not appear in the present cured samples. The samples synthesised by the conventional method contain a sharp resonance at −81 ppm (Fig. 3e); this is the position of the resonance reported for zeolite Li-ABW [22], confirming the XRD identification of this as the principal product of the conventional synthesis. All the samples synthesised by the solid-state methods contain a principal sharp resonance at −85.3–85.7 ppm (Fig. 3f–h) and a weak resonance near −90 ppm, both attributable to zeolite Li-EDI [23]. The solid-state samples contain, in addition to this peak, another at about −107 ppm (Fig. 3f–h) indicating the presence of unreacted silica. Sample M4, which is shown by XRD to contain, in addition to zeolite Li-EDI the zeolites A and X, shows a more complex spectrum (Fig. 3h) in which the principal resonance at −85.7 ppm contains a contribution from Li zeolite A [24], and shoulders at about −84 and −96 ppm corresponding to Li-zeolite X [24]. The sharp resonance at −74.7 ppm arises from the unreacted Li_2SiO_3 also present [25].

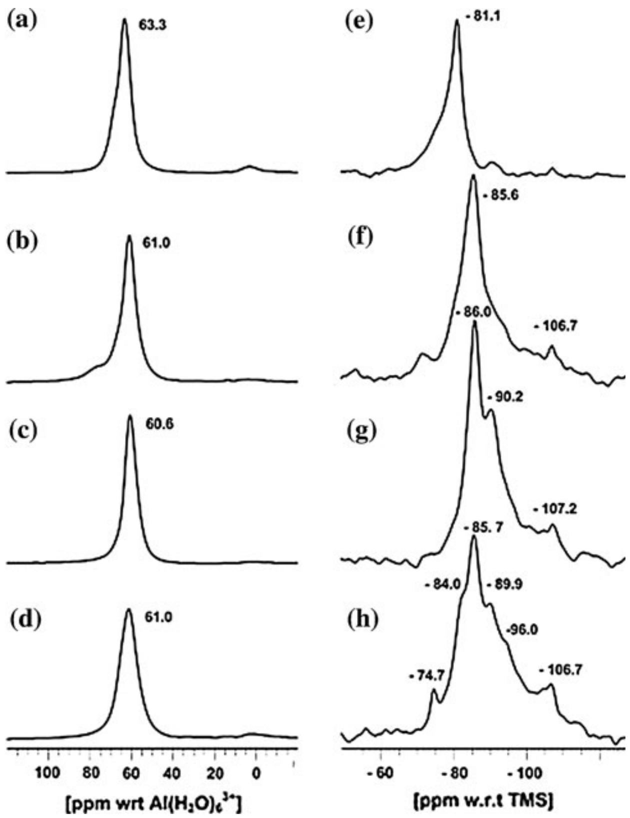

Fig. 3 Typical 11.7T ^{27}Al and ^{29}Si MAS NMR spectra of cured lithium inorganic polymers. **a**, **e** Sample C1, **b**, **f** sample S, **c**, **g** sample M1, **d**, **h** sample M4

Effect of heat treatment

All the monolithic samples heated at 800 °C were weak, but heating at 900 °C caused the solid-state samples S and M1 and the conventionally synthesised samples C1–C3 to densify. After heating to 1100 °C most of the samples retained their strength, but some developed hairline cracks. The samples prepared by the alternative solid-state synthesis method using silica fume developed 0.5-mm orange specks on heating, presumably due to the formation of kunzite and/or iron impurities [26, 27].

XRD of the samples heated at 800–1275°C (not shown) indicated that the principal phase in all cases was β-eucryptite (PDF no. 45-0467). β-spodumene (PDF no. 35-0797) was also present as a minor product in many of the samples. Sample S heated at 800 °C contained a small amount of β-spodumene, while samples M1–M4 contained quartz which reacted at 900 °C to form small amounts of β-spodumene. This subsequently decomposed at 1100 °C to highly crystalline β-eucryptite. On heating to 1275 °C, samples M2–M4 formed increasing amounts of β-spodumene, whereas samples C1–C3 melted.

The microstructures of the solid-state samples S and M1–M4 heated to 1100 °C (Fig. 4) become progressively less homogeneous with increasing silica content. Samples C1 (Fig. 4a), S (Fig. 4b) and M1 (Fig. 4c) consist mainly of a homogeneous glassy matrix with no crystallites visible up to ×5000 magnification, suggesting that any crystallites present will be of submicron size. Sample M2 (not shown) contains 10-µm crystallites in a glassy matrix. Samples M3 and M4 (Fig. 4d) contain 1-µm grains showing signs of incipient sintering (Fig. 4b).

The microstructural differences in the heated samples appear to be due to the formation of a glassy lithium silicate phase. The 1:1 Si/Al ratio of Li-EDI implies the existence of some unreacted SiO_2. In samples containing less SiO_2 the relatively higher Li_2O content facilitates the formation of a low-temperature eutectic, as confirmed by the disappearance of the quartz in samples S and M1–M4 as the temperature is increased from 800 to 900 °C. Samples C1–C3 contain more Li_2O than is required to form

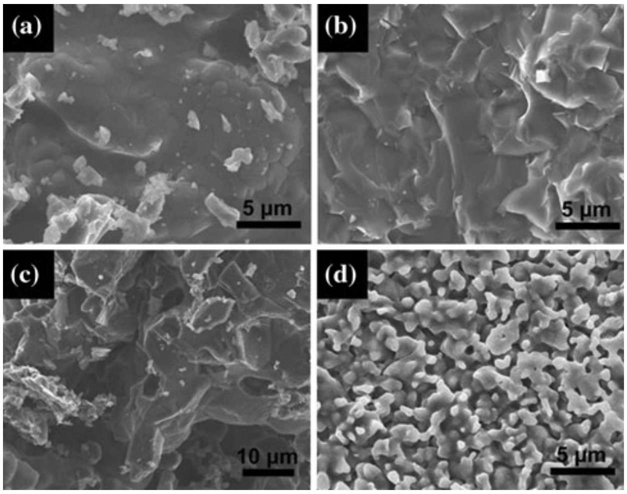

Fig. 4 SEM images of lithium aluminosilicates heated at 1100 °C. **a** Sample C1, **b** sample S, **c** sample M1, **d** sample M4

β-eucryptite, giving rise to the crystalline Li_2SiO_3 observed in these samples at 800 and 900 °C. The difference in strength between sample S and the other samples heated to 900 °C may be due to lack of phase changes in sample S, apart from the loss of quartz and the formation of a glassy phase. Alternatively, since sample S contains significantly less silica than the other samples, it may form less inhomogeneous material, resulting in a stronger fired product.

The phase formation sequence upon heating the present lithium aluminosilicates may therefore be summarised as follows:

(1) initial formation of β-eucryptite at <800 °C,
(2) reaction of the unreacted silica-rich regions at 900 °C to form β-spodumene,
(3) decomposition of β-spodumene at 1100 °C to form additional β-eucryptite,
(4) in samples of higher silica content, the reappearance at 1275 °C of β-spodumene, the thermodynamically favoured phase in these samples.

The microstructures of samples S and M1 are quite homogeneous with relatively little debris and, although, XRD indicates the presence of crystalline products. The existence of very fine crystallites in the heated products suggests that the present precursors could provide a useful route to thermal shockproof lithium aluminosilicate materials. Although the mechanical properties of articles manufactured in this manner are likely to be inferior to conventional glass-ceramics because of their porosity and relative inhomogeneity, they may be competitive because of their relatively low-firing temperatures, cheap precursor materials and simple synthesis equipment, and their ability to be cast to shape prior to firing.

Conclusions

1. Syntheses of lithium aluminosilicate inorganic polymers were carried out by the three different methods; (i) a synthesis similar to that of conventional sodium or potassium geopolymers in which dehydroxylated halloysite clay was reacted under highly alkaline conditions with lithium hydroxide or lithium silicate solutions of two different Li_2O/SiO_2 molar ratios, (ii) a solid state reaction in which dehydroxylated halloysite was reacted with LiOH at 550 °C for 4 h and the solid reaction product hydrated by the addition of water, (iii) a modified solid-state synthesis in which solid lithium silicates of four different compositions, prepared by reaction of LiOH with fine silica fume powder at 600 °C, were dry-mixed with dehydroxylated halloysite then hydrated by the addition of water. The compositions of the materials prepared by all the three methods were similar, and corresponded to those previously reported to produce viable geopolymers.
2. After curing at 40 °C, all three synthesis methods hardened to form solid samples with physical properties depending on the amount of water used, the most viable being samples synthesised with H_2O/Li_2O molar ratios ranging from 9 to 10.
3. None of the cured materials showed the amorphous XRD pattern characteristic of a true geopolymer, but contained lithium zeolites, principally the lithium zeolite Li-ABW in the conventionally synthesised materials, and the fibrous edingtonite-structured zeolite Li-EDI in the compounds formed by the solid-state syntheses. The formation of Li-EDI may be favoured by the lower pH conditions of the solid-state syntheses. These XRD results were confirmed by ^{27}Al and ^{29}Si MAS NMR spectroscopy.
4. On heating at 800–1275 °C, a series of compounds is formed. The principal crystalline compound formed in all the samples <800 °C is β-eucryptite, $LiAlSiO_4$. At 900 °C, the unreacted silica-rich regions form β-spodumene, $LiAlSi_2O_6$ which decomposes at 1100 °C to form additional β-eucryptite. At 1275 °C, β-spodumene reappears in the samples of higher silica content.

Judicious manipulation of the composition and thermal treatment of the Li-zeolites resulting from these syntheses could make them useful precursors to β-eucryptite and β-spodumene ceramics.

Acknowledgements We are indebted to M. J. Ryan for assistance with the interpretation of the XRD data and to D. Flynn for assistance with the electron microscopy. This study was partly funded by a subcontract from Industrial Research Ltd. of the Foundation for Research Science and Technology contract CO8X0302 and partly by the MacDiarmid Institute for Advanced Materials and Nanotechnology.

References

1. Davidovits J (1991) J Therm Anal 37:1633
2. Barbosa VFF, MacKenzie KJD, Thurmaturgo C (2000) Int J Inorg Mater 2:309
3. Iler RK (1979) The chemistry of silica. Wiley, New York
4. Wijnen PWJG (1989) J Non-Cryst Sol 109:85
5. Kinrade SD, Pole DL (1992) Inorg Chem 31:4558
6. Fletcher RA, MacKenzie KJD, Nicholson CL, Shimada S (2005) J Eur Ceram Soc 25:1471
7. Barrer RM, Mainwaring DE (1972) J Chem Soc Dalton Trans 2534
8. Barbosa VFF, MacKenzie KJD (2003) Mater Lett 57:1477
9. Cundy CS, Cox PA (2005) Microporous Mesoporous Mater 82:1
10. Kolousek D, Brus J, Urbanova M, Andertova J, Hulinsky V, Vorel J (2007) J Mater Sci 42:9267. doi:10.1007/s10853-007-1910-5
11. MacKenzie KJD (2009) Ceram Eng Sci Proc 30:251
12. Beall GH (1992) Ann Rev Mater Sci 22:91
13. Roy R, Agrawal DK, McKinstry HA (1989) Ann Rev Mater Sci 19:59
14. Bedard RL, Flanigen EM (1993) United States Patent 5179051
15. Subramanian MA, Corbin DR, Chowdhry U (1993) Bull Mater Sci 16:665
16. Baerlocher C, Meier WM, Olson DH (2001) Atlas of zeolite framework types, 5th edn. Elsevier, Amsterdam
17. Matsumoto T, Miyazaki T, Goto Y (2006) J Eur Ceram Soc 26:455
18. Sathupunya M, Gulari E, Wongkasemjit S (2004) Mater Chem Phys 83:89
19. Yao ZT, Xia MS, Ye Y, Zhang L (2009) J Hazardous Mater 170:639
20. Haden WL, Dzierzanowski F (1964) United States Patent 3123441
21. Rees CA, Provis JL, Lukey GC, van Deventer JSJ (2008) Colloids Surf A 318:97
22. Klinowski J, Thomas JM, Fyfe CA, Hartman JS (1981) J Phys Chem 85:2590
23. Rios CA, Williams RCD, Roberts CL (2009) Fuel 88:1403
24. Klinowski J (1984) Prog Nucl Magn Reson Spectrosc 16:237
25. Magi M, Lippmaa E, Samosan A (1984) J Phys Chem 88:1518
26. Gabriel A, Slavin M, Carl HF (1942) Econom Geol 37:116
27. Yamuna A, Devanarayanan S, Lalithambika M (2001) J Am Ceram Soc 84:1703